Fréedericksz transition in polymer-stabilized nematic liquid crystals

Rui-Qing Ma and Deng-Ke Yang
Liquid Crystal Institute and Chemical Physics Program, Kent State University, Kent, Ohio 44242
(Received 20 May 1999)

We have constructed polymer-stabilized nematic liquid crystals by photopolymerizing diacrylate monomers in the nematic phase. The orientation of the liquid crystal was controlled by the polymer network. We studied the Fréedericksz transition in these systems. Experimentally we studied the transition by measuring the capacitance of the liquid crystal cells as a function of applied voltage. The transition was affected profoundly by the dispersed polymer network. The threshold was higher with shorter interpolymer network distance. Theoretically we studied the systems using a two-dimensional model in which the polymer networks were represented by parallel cylinders with random location. The interaction between the liquid crystal and the polymer network was described by the boundary condition imposed by the polymer network. By fitting the experimental data, we found that the polymer cylinders had diameters of a few submicrons, and a substantial amount of liquid crystal was trapped inside the cylinders.

PACS number(s): 61.30.Cz, 64.70.Md, 64.75.+g

INTRODUCTION

Polymer-stabilized liquid crystals are composites with small amounts of polymer networks dispersed in liquid crystals [1–5]. They are heterogeneous systems and have attracted a lot of attention in the past few years. Polymer stabilization is also a very useful technique in applications. Desired properties, not possible with surface alignments, have been achieved using this technique [6–11]. A polymer-stabilized liquid crystals is constructed by mixing a small amount of bifunctional monomer and liquid crystal. When the monomer is polymerized, the mixture is in a liquid crystal phase such as nematic, cholesteric, or smectic. During the polymerization, the environment for the monomers is anisotropic because the liquid crystal possesses anisotropic properties. The liquid crystal has an aligning effect on the monomers and the diffusion of the monomers is anisotropic. Because of these two factors, fibril-like and anisotropic polymer networks are formed. The polymer network mimics the structure of the liquid crystal to some extent [6]. It has an aligning effect on the liquid crystal and, in turn, can be used to control the orientation of the liquid crystal.

It is important to study the morphology of the polymer networks formed in liquid crystals and to understand the relation between the morphology and the polymerization conditions. The morphology of a polymer network is determined by the chemical structure of the monomer and the process of phase separation, which is affected by the polymerization conditions. The interaction between polymer networks and liquid crystals depends on the morphology of the polymer network. Understanding the morphology of the polymer network helps us to understand phase separation and also enables better use of polymer networks in applications. Several experimental techniques have been used to study the morphology of the networks in polymer-stabilized liquid crystals. Scanning electron microscopy (SEM) was used to observe directly the polymer network after the liquid crystal was extracted. It was observed that the polymer network was fibril-like with fibril lateral size of a few tenths of a micron [6,12,13]. There was concern, however, that the observed fibrils might be different from the polymer network before the liquid crystal was extracted, because the polymer network might have collapsed during the extraction. Confocal microscopy also showed that the fibrils of the polymer network had a lateral size of a few tenths of a micron, but the image was not very sharp [14]. Birefringence is another technique that has been used to study polymer-stabilized liquid crystals [15,16]. When the temperature was raised from the nematic phase to the isotropic phase, the orientational order of the polymer network was retained because the network was a cross-linked polymer. The polymer network induced a nematic order in the liquid crystal nearby. Both the polymer network and the liquid crystal with induced order contributed to the birefringence of the material. The induced birefringence depended on the surface area of the polymer network, which in turn depended on the lateral size of the polymer fibril when the concentration of the polymer was fixed. By measuring and modeling the birefringence of the polymer-stabilized liquid crystal, the lateral size of the polymer fibril was found to be a few nanometers.

In order to explain the experimental results, a fibril-bundle model was proposed for the polymer network in a polymer-stabilized liquid crystal: (1) a few polymer molecular chains form a fibril of lateral size of a few nanometers; (2) hundreds of fibrils and some trapped liquid crystal form a bundle with lateral size around a few tenths of a micron and distance between the fibrils of a few nanometers [15]. The fibril-bundle model of the polymer network is shown in Fig. 1. Scanning electron microscopy and confocal microscopy were used to detect the polymer bundles. In the birefringence study, the induced birefringence was mainly from the liquid crystal trapped inside the bundle and therefore the birefringence study was sensitive only to the lateral size of the polymer fibrils.

In this paper we report the results of a study on the Fréedericksz transition in polymer-stabilized nematic liquid crystals. The transition was studied by measuring the capacitance of the liquid crystal cells. At the electric field we applied, the liquid crystal between the polymer bundles reoriented but not the liquid crystal trapped inside the bundles. As we will

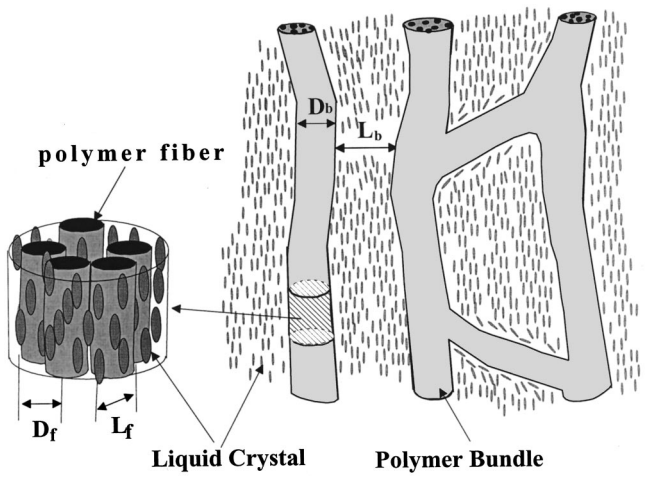

FIG. 1. Schematic diagram showing the bundle model for the polymer network formed in a nematic liquid crystal.

show, the threshold and the capacitance-voltage (C-V) curve depend on the lateral size of the bundles and the distance between the bundles. By measuring and modeling the capacitance-voltage curve, we were able to find the lateral size of the bundles, the distance between the bundles, and the percentage of the liquid crystal trapped inside the bundles.

THEORETICAL MODELING

We studied theoretically a polymer-stabilized nematic liquid crystal system with homogeneous orientation. The liquid crystal has a positive dielectric anisotropy ($\Delta\varepsilon=\varepsilon_{\parallel}-\varepsilon_{\perp}>0$). At zero field, the liquid crystal and the polymer network are unidirectionally aligned parallel to the cell surface (in the x direction), and the cell has the minimum capacitance. When a sufficiently high voltage is applied across the cell, the liquid crystal between the polymer bundles is reoriented by the field to be perpendicular to the cell surface (in the z direction) while the polymer network and the liquid crystal trapped inside it remain in the x direction. In the simulation we simplified the polymer bundles as parallel square prisms as shown in Fig. 2. They were assumed to be of the same size with circumference length $4D_b$ and were randomly located as shown in Fig. 3. This is a two-dimensional problem (in the yz plane). The thickness of the cell is H. The length we consider in the y direction is L. There are N polymer bundles inside the area defined by HL. The average distance between the polymer bundles is calculated as $L_b=(HL/N)^{0.5}$. The volume fraction of the bundles

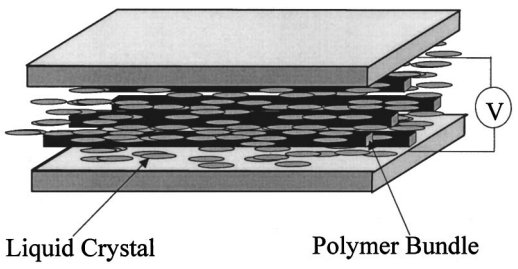

FIG. 2. Schematic diagram of the simplified model of polymer bundles used in modeling the capacitance-voltage curve in the Fréedericksz transition in polymer-stabilized liquid crystals.

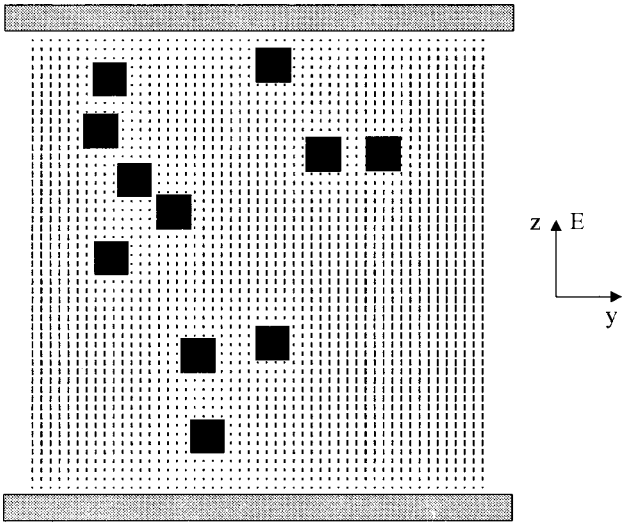

FIG. 3. Liquid crystal director on the cross section perpendicular to the polymer bundles when a sufficiently high voltage is applied.

(including the liquid crystal trapped inside them) is v_f, where

$$v_f=\frac{ND_b^2}{HL}. \tag{1}$$

The liquid crystal director $\vec{n}$ is in the xz plane. At zero voltage, $\vec{n}$ is along the $\hat{\mathbf{x}}$ direction. When the voltage V is applied, $\vec{n}$ is tilted to the $\hat{\mathbf{z}}$ direction. The angle between $\vec{n}$ and $\hat{\mathbf{x}}$ is θ. θ is a function of y and z, that is, $\theta=\theta(y,z)$. The electric field has only a z component, $\vec{E}=E(y,z)\hat{\mathbf{z}}$. The z component of the electric displacement $\vec{D}$ is a constant independent of z, given by

$$D_z=\varepsilon_0\varepsilon_{\perp}[1+\Delta\varepsilon\sin^2\theta(y,z)]E(y,z)=\sigma(y), \tag{2}$$

where σ is the surface charge density, a function of y and $\Delta\varepsilon=(\varepsilon_{\parallel}-\varepsilon_{\perp})/\varepsilon_{\perp}$. The voltage applied across the cell is the same at any position, independent of y,

$$V=\int_0^H E(y,z)dz=\int_0^H\frac{\sigma(y)}{\varepsilon_0\varepsilon_{\perp}[1+\Delta\varepsilon\sin^2\theta(y,z)]}dz. \tag{3}$$

For the purpose of simplicity, it is assumed that the polymer has the same dielectric tensor as the liquid crystal. This does not produce too much error because the concentration of the polymer is usually less than 5 wt %. The average capacitance C of unit area of the cell is calculated from

$$C=\frac{1}{V}\left(\frac{1}{L}\int_0^L\sigma(y)dy\right). \tag{4}$$

In our calculation, L was chosen large enough to give a stable average value of the capacitance.

The components of the liquid crystal director $\vec{n}$ are

$$n_x=\cos\theta(y,z),\quad n_y=0,\quad n_z=\sin\theta(y,z). \tag{5}$$

The elastic energy density of the liquid crystal was found to be

$$f_{\mathrm{ela}}=\frac{1}{2}(K_{11}\cos^2\theta+K_{33}\sin^2\theta)\left(\frac{\partial\theta}{\partial z}\right)^2+\frac{1}{2}K_{22}\left(\frac{\partial\theta}{\partial y}\right)^2. \tag{6}$$

The electric energy density of the liquid crystal is given by [17]

$$f_{\mathrm{ele}}=\frac{1}{2}\vec{E}\cdot\vec{D}=\frac{1}{2}ED_z=\frac{\sigma^2(y)}{2\varepsilon_0\varepsilon_\perp(1+\Delta\varepsilon\sin^2\theta)}. \tag{7}$$

The following dimensionless variables are introduced:

$$\xi=\frac{z}{H},\quad \eta=\frac{y}{H},\quad K_1=\frac{K_{11}}{K_{22}},\quad K_3=\frac{K_{33}}{K_{22}},\quad R=\frac{\sigma^2H^2}{\varepsilon_0\varepsilon_\perp K_{22}}. \tag{8}$$

Minimizing the total free energy with a given $\sigma(y)$, we obtain

$$\frac{\partial^2\theta}{\partial\eta^2}+(K_1\cos^2\theta+K_3\sin^2\theta)\frac{\partial^2\theta}{\partial\xi^2}+(K_3-K_1)\times\sin\theta\cos\theta\left(\frac{\partial\theta}{\partial\xi}\right)^2+\frac{R\Delta\varepsilon\sin\theta\cos\theta}{(1+\Delta\varepsilon\sin^2\theta)^2}=0. \tag{9}$$

An over-relaxation numerical method is used to find the solution for Eq. (9). In the simulation we use the following strategy: For a given value of the surface charge density $\sigma(y=0)$ at $y=0$, the voltage across the cell at $y=0$ is calculated as

$$V(y=0)=\int_0^H\frac{\sigma(0)}{\varepsilon_0\varepsilon_\perp[1+\Delta\varepsilon\sin^2\theta(0,z)]}dz.$$

At any other place y, the surface charge density $\sigma(y)$ is adjusted so that the voltage across the cell is the same everywhere, that is, $V(y)=V(y=0)$.

The surface anchoring on the cell surface is assumed to be infinitely strong. The boundary condition at the cell surface is

$$\theta(z=0)=0,\quad \theta(z=H)=0. \tag{10}$$

A periodic boundary condition is used at $y=0$ and $y=L$. On the polymer bundle surface, it is assumed that the polar anchoring strength and the azimuthal anchoring strength have the same value W. The surface anchoring energy density is

$$f_s=\tfrac{1}{2}W\sin^2\theta. \tag{11}$$

The boundary condition on the surface of the polymer bundle parallel to the cell surface is

$$\frac{\partial\theta}{\partial\xi}=\pm\frac{H}{d_a}\frac{\sin\theta\cos\theta}{(K_1\cos^2\theta+K_3\sin^2\theta)}, \tag{12}$$

where $d_a=K_{22}/W$ is the anchoring extrapolation length, $+$ is for the top surface and $-$ for the bottom surface. The boundary condition on the surface of the polymer bundle perpendicular to the cell surface is

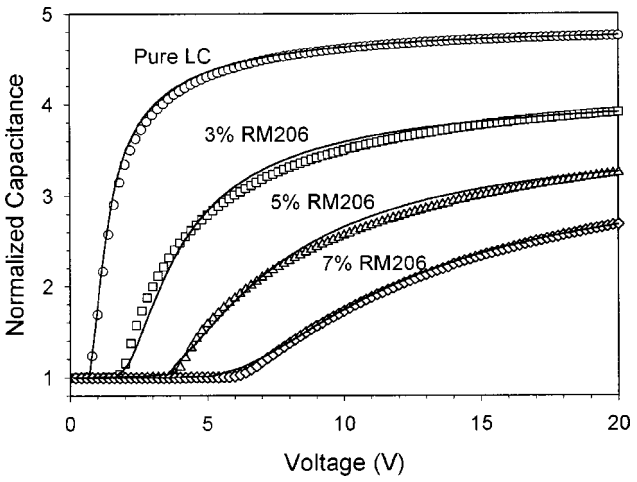

FIG. 4. Capacitance-voltage curves in the Fréedericksz transition in polymer-stabilized nematic liquid crystal samples with different polymer concentrations. Points: experimental data; solid line: theoretical fitting.

$$\frac{\partial\theta}{\partial\eta}=\pm\frac{H}{d_a}\sin\theta\cos\theta, \tag{13}$$

where $+$ is for the right side surface and $-$ for the left.

In the experiment, a liquid crystal with known dielectric constants and elastic constants was used. In fitting the experimental results, the fitting parameters were the volume fraction of the polymer bundle v_f, the size of the bundle D_b, and the surface anchoring strength on the surface of the polymer bundle W. In the calculation of the C-V curve, v_f and D_d affected the threshold of the Fréedericksz transition and the part of the C-V curve at voltages near the threshold W affected the C-V curve at intermediate voltages, and v_f affected the C-V curve at high voltages.

EXPERIMENT AND RESULTS

The polymer-stabilized nematic liquid crystal was a mixture of nematic liquid crystal ZLI4469-100 (from Merck), diacrylate monomer RM206 (from Merck), and photoinitiator BME (bezoin methyl ether, from Polyscience). The concentration of the monomer was 5 wt% unless otherwise specified. The ratio between the concentration of RM206 and that of BME was 10:1. The liquid crystal had the following parameters: $K_{11}=10.0\times10^{-12}$ N, $K_{22}=6.3\times10^{-12}$ N, $K_{33}=13.9\times10^{-12}$ N, $\varepsilon_\parallel=29.8$, and $\varepsilon_\perp=6.1$. RM206 has a rigid core and flexible tails like liquid crystal molecules. The mix-

TABLE I. Threshold and fitting parameters for the Fréedericksz transition in polymer-stabilized nematic liquid crystal samples with different polymer concentrations.

Polymer concentration (%)	V_{th} (V)	V_f (%)	Trapped liquid crystal (%)	D_b (nm)	L_b (nm)
0	0.7				
3	1.95	5.0	40	527	2356
5	3.8	9.0	44	428	1426
7	6.1	11.7	40	308	900

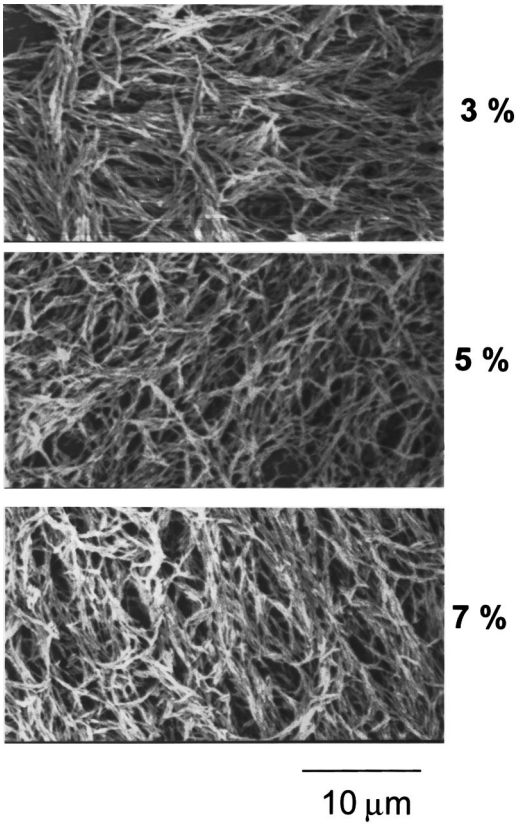

FIG. 5. SEM pictures of polymer bundles in polymer-stabilized nematic liquid crystal samples with different polymer concentrations.

ture was in the nematic phase at room temperature. It was introduced into cells consisting of two parallel glass plates with thickness controlled by glass spacers. The cells had antiparallel rubbed polyimide alignment layers with pretilt angle less than 1°. The cells were irradiated with uv light for photopolymerization. The uv intensity was 12 mW/cm^2 unless otherwise specified. The uv curing time was 30 min. The curing was at room temperature unless otherwise specified.

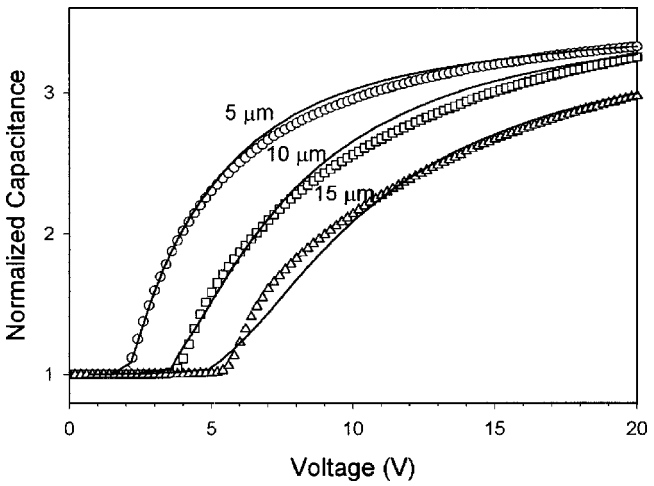

FIG. 6. Capacitance-voltage curves in the Fréedericksz transition in polymer-stabilized nematic liquid crystal samples with different cell thicknesses. Points: experimental data; solid line: theoretical fitting.

TABLE II. Threshold and fitting parameters for the Fréedericksz transition in polymer-stabilized nematic liquid crystal samples with different cell thicknesses.

Cell thickness (μm)	V_{th} (V)	v_f (%)	Trapped liquid crystal (%)	D_b (nm)	L_b (nm)
5	2.0	12.2	59	526	1506
10	3.8	9.0	44	428	1426
15	5.4	9.5	47	464	1505

The Fréedericksz transition was studied using a HP 4284A *LCR* meter. The frequency of the applied voltage was 1 kHz. The applied voltage was varied at the rate of 0.04 V/s. The maximum applied voltage was 20 V, the highest voltage that can be provided by the *LCR* meter. The result was the same for increasing and decreasing voltage.

After the Fréedericksz transition study, the samples were prepared for SEM study. The cells were split using a razor blade and then were immersed in hexane for a few minutes to extract the liquid crystal. The polymer network was left behind on the glass plate and was coated with gold for SEM.

A. Samples with different polymer concentrations

We first studied the effects of the polymer concentration. The cell thickness was fixed at 10 μm. The experimental results are shown in Fig. 4. The experimental data are indicated by symbols and the calculated data are represented by solid lines. As the polymer concentration was increased, the

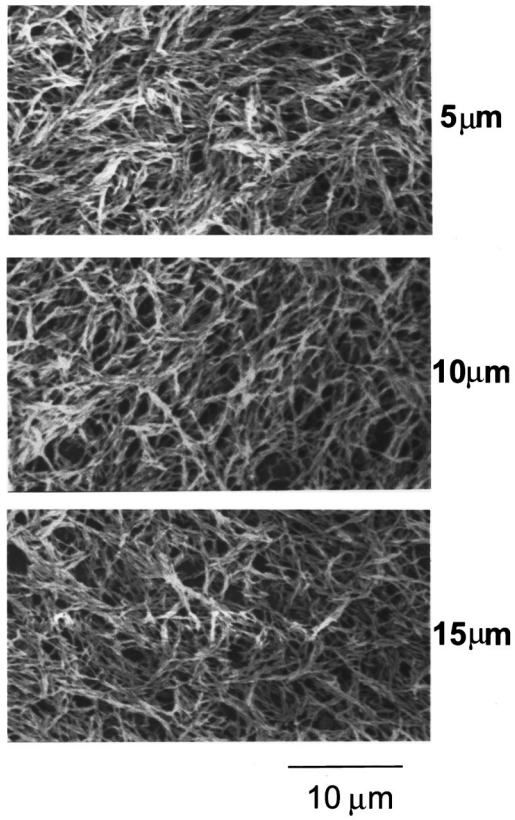

FIG. 7. SEM pictures of polymer bundles in polymer-stabilized nematic liquid crystal samples with different cell thicknesses.

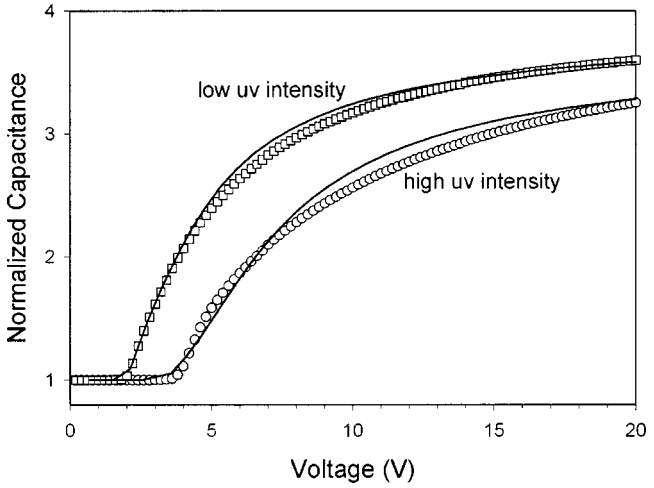

FIG. 8. Capacitance-voltage curves in the Fréedericksz transition in polymer-stabilized nematic liquid crystal samples cured with different uv intensities. Points: experimental data; solid line: theoretical fitting.

threshold V_{th} of the Fréedericksz transition was shifted higher because the distance between the polymer bundles was decreased. The fitting parameters were volume fraction v_f, the width of the square prime D_b, and the surface anchoring strength W. The concentration x_p indicated in the figure is the concentration of the polymer, i.e., the weight concentration of the monomer, but not the volume fraction v_f of the polymer bundle, which contained some liquid crystal. It was assumed that the densities of the monomer and the liquid crystal were the same. The fitting parameters v_f and D_b are listed in Table I. The volume fraction v_f is larger than the polymer concentration x_p. The percentage of the trapped liquid crystal is the percentage of the volume of the liquid crystal inside the polymer bundle. For example, when the polymer concentration was 3%, the volume fraction of the polymer bundle was 5%. That means that the polymer bundle consisted of 60% polymer fibril and 40% liquid crystal. As the polymer concentration was increased, the fitting showed that the lateral size of the bundle decreased. The SEM pictures of the samples are shown in Fig. 5. It can be seen that the polymer bundles have lateral sizes of a few tenths of a micron, and the lateral size of the bundles seems independent of the polymer concentration. This discrepancy for the lateral size of the bundle between the results of fitting the capacitance-voltage curve and the SEM study may be attributed to there being more polymer near the cell surfaces than in the bulk, as observed by SEM study [18]. If the amount of polymer formed near the cell surfaces was fixed,

TABLE III. Threshold and fitting parameters for the Fréedericksz transition in polymer-stabilized nematic liquid crystal samples cured with different uv intensities.

uv intensity (mW/cm^2)	V_{th} (V)	v_f (%)	Trapped liquid crystal (%)	D_b (nm)	L_b (nm)
0.04	2.1	8.0	38	706	2496
12	3.8	9.0	44	428	1426

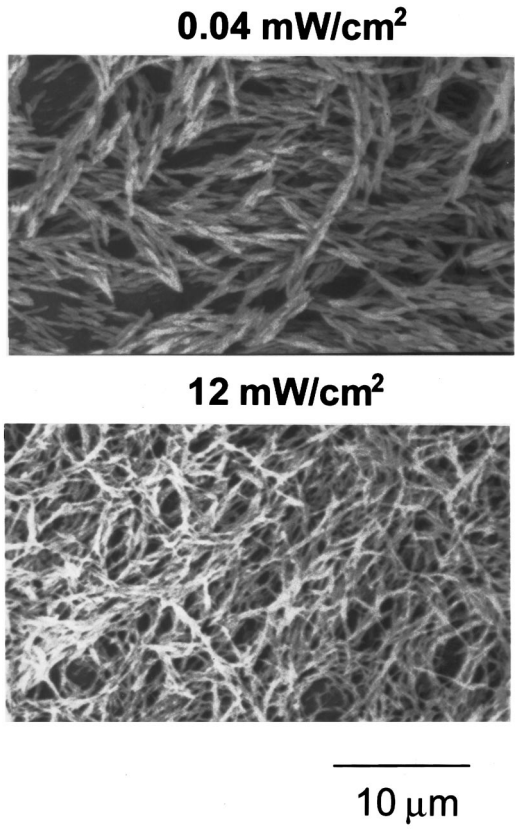

FIG. 9. SEM pictures of polymer bundles in polymer-stabilized nematic liquid crystal samples cured with different uv intensities.

the percentage (with respect to the total polymer concentration) of polymer network in the bulk was lower when the polymer concentration was lower. In order to fit the capacitance-voltage curve, a bundle smaller than the value listed in Table I had to be used when the polymer concentration was lower. Then the difference between bundle sizes with different polymer concentration will be smaller. Calculation shows that if there is 1.8% polymer at the cell surface,

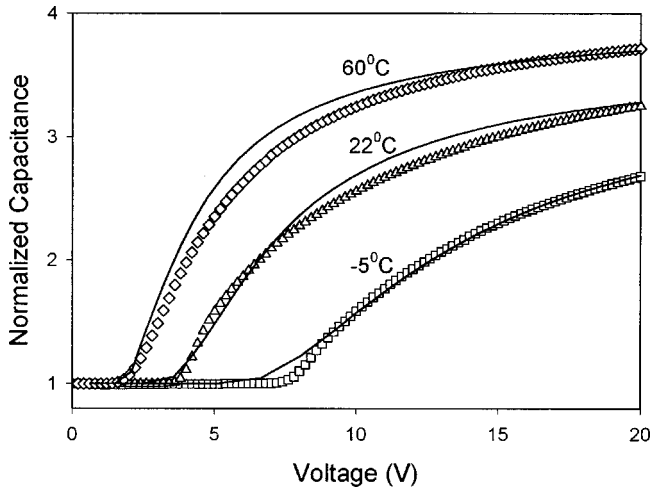

FIG. 10. Capacitance-voltage curves in the Fréedericksz transition in polymer-stabilized nematic liquid crystal samples cured at different temperatures. Points: experimental data; solid line: theoretical fitting.

TABLE IV. Threshold and fitting parameters for the Fréedericksz transition in polymer-stabilized nematic liquid crystal samples cured at different temperatures.

Curing temperature (°C)	V_{th} (V)	v_f (%)	Trapped liquid crystal (%)	D_b (nm)	L_b (nm)
−5	7.6	10.8	54	244	371
22	3.8	9.0	44	428	1426
60	1.8	7.0	29	662	2502

then samples with different polymer concentrations will have the same bundle size of 350 nm.

Regarding the surface anchoring W on the surface of the polymer bundle, when it was equal to or larger than $1.5\times10^{-4} j\ m^{-2}$, good fitting was obtained. This value is comparable to that of the rubbed polyimide surface.

The fitting parameters were obtained by visually fitting the calculated curve to the experimentally measured curve. When the fitting parameters were varied by ±10%, the fitting curve became significantly different from the measured curve, so the relative error of the fitting parameters listed in the tables is about ±10%.

B. Samples with different cell thicknesses

We studied polymer-stabilized nematic liquid crystals in cells with various thicknesses. The polymer concentration was fixed at 5%. The experimentally measured capacitance-voltage curves are shown by the points in Fig. 6. The threshold increases with cell thickness. Without the polymer network, the orientation of the liquid crystal was imposed by the anchoring of the two cell surfaces; and the voltage threshold is a constant independent of the cell thickness. In the polymer-stabilized nematic liquid crystal, the orientation of the liquid crystal is imposed by the polymer bundles and the distance (~1.5 μm) between the polymer bundles is much smaller than the cell thickness. As expected, the threshold is approximately linearly proportional to the cell thickness. The fitting parameters are listed in Table II. The lateral size of the polymer bundle is approximately independent of the cell thickness. The SEM pictures are shown in Fig. 7, and the lateral size of the polymer bundles are approximately the same.

C. Samples cured with different uv intensities

The intensity of the uv irradiation is a factor affecting polymerization. We prepared two polymer-stabilized nematic liquid crystal samples with uv intensities of 0.04 and 12 mW/cm^2, respectively. The curing time was 4 h when the uv intensity was 0.04 mW/cm^2. The cell thickness was 10 μm and the polymer concentration 5%. The experimentally measured capacitance-voltage curves are shown in Fig. 8. The fitting parameters are listed in Table III. As expected, at lower curing uv intensity, there are fewer activated photoinitiators; the polymer bundles grow larger. The lateral size of the polymer bundles given by the fitting agrees with the SEM pictures shown in Fig. 9. At low curing uv intensity, there is also less liquid crystal trapped in the bundles.

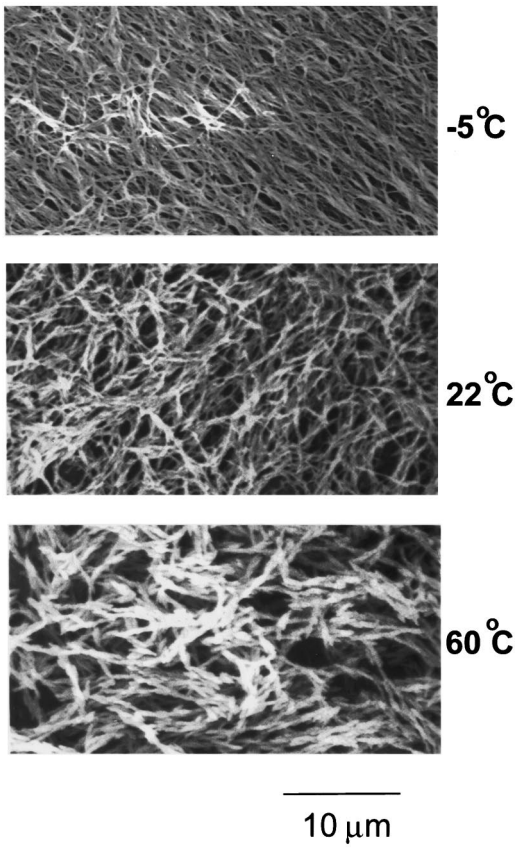

FIG. 11. SEM pictures of polymer bundles in polymer-stabilized nematic liquid crystal samples cured at different temperatures.

D. Samples cured at different temperatures

The temperature at which polymerization took place was another factor affecting the polymer network. We prepared samples at three temperatures. The cell thickness was 10 μm and the polymer concentration was 5%. The experimental measured and simulated capacitance-voltage curves are shown in Fig. 10. The fitting parameters are listed in Table IV. At higher curing temperature, the diffusion of the monomers is faster, and in the phase separation, more polymer fibrils can get together to form larger bundles. This tendency is also confirmed by the SEM pictures shown in Fig. 11. Furthermore, at higher curing temperature, the Fréedericksz transition study shows that less liquid crystal is trapped in the polymer bundles.

CONCLUSION

We have studied the Fréedericksz transition in polymer-stabilized liquid crystals. Our results support the bundle model of the polymer network formed in liquid crystals. By fitting the experimentally measured capacitance-voltage curves, we were able to determine the size of the polymer bundle, the amount of liquid crystal trapped inside the bundle, and the anchoring strength of the bundle surface. The lateral size of the polymer bundle was found to be a few tenths of a micron, which was confirmed by SEM. The bundle consisted of approximately equal amounts of polymer

fibrils and liquid crystal molecules. Our results also showed that smaller polymer bundles can be formed by using higher curing uv irradiation intensity or lower curing temperature. Because of the good agreement between the experimental data and the results of the theoretical modeling, we conclude that the interaction between the liquid crystal and the polymer network can be described in terms of the boundary condition imposed by the polymer network.

ACKNOWLEDGMENT

This research was supported by NSF under ALCOM Grant No. DMR89-20147.

[1] D. Broer, R. Gossink, and R. Hikmet, Angew. Makromol. Chem. **183**, 45 (1990).
[2] R. A. M. Hikmet, Liq. Cryst. **9**, 405 (1991).
[3] D.-K. Yang, L.-C. Chien, and J. W. Doane, Appl. Phys. Lett. **60**, 3102 (1992).
[4] S. I. Stupp, S. Son, H. C. Lin, and L. S. Li, Science **259**, 59 (1993).
[5] G. P. Crawford and S. Zumer, in *Liquid Crystals in Complex Geometries Formed by Polymer and Porous Networks*, edited by G. P. Crawford and S. Zumer (Taylor & Francis, London, 1996).
[6] Y. K. Fung, D.-K. Yang, Y. Sun, L. C. Chien, S. Zumer, and J. W. Doane, Liq. Cryst. **19**, 797 (1995).
[7] Y. Fung, D. K. Yang, and J. W. Doane, in *Eurodisplay '93 Conference Proceedings*, (Society for Information Display, 1993), p. 157.
[8] D.-K. Yang, J. L. West, L. C. Chien, and J. W. Doane, J. Appl. Phys. **76**, 1331 (1994).
[9] P. Bos, J. Rahman, and J. W. Doane, SID Int. Symp. Dig. Tech. Pap. **24**, 877 (1993).
[10] J. Pins, R. Blinc, B. Martin, S. Pirs, and J. W. Doane, Mol. Cryst. Liq. Cryst. Sci. Technol., Sect. A **264**, 155 (1995).
[11] R. A. M. Hikmet, J. Appl. Phys. **68**, 4406 (1990).
[12] I. Dierking, L. L. Kosbar, A. Afzali-Ardakani, A. C. Lowe, and G. A. Held, J. Appl. Phys. **81**, 3007 (1997).
[13] C. V. Rajaram, S. D. Hudson, and L. C. Chien, Chem. Mater. **8**, 2451 (1996).
[14] G. A. Held, L. L. Kosbar, I. Dierking, A. C. Lowe, G. Grinstein, V. Lee, and R. D. Miller, Phys. Rev. Lett. **79**, 3443 (1997).
[15] Y. K. Fung, A. Borstnik, S. Zumer, D.-K. Yang, and J. W. Doane, Phys. Rev. E **55**, 1637 (1997).
[16] R. E. Kraig, P. L. Taylor, R. Q. Ma, and D.-K. Yang, Phys. Rev. E **58**, 4594 (1998).
[17] R. Barberi and G. Barnero, in *Physics of Liquid Crystalline Materials*, edited by I. C. Khoo and F. Simoni (Gordon and Breach, Philadelphia, 1988).
[18] R.-Q. Ma and D.-K. Yang, Tech. Rep. ALCOM Symp. **X**, 73 (1998).